Acoustic metamaterials with coupled local resonators for broadband vibration suppression

Guobiao Hu, Lihua Tang, Raj Das, Shiqiao Gao, and Haipeng Liu

Citation: AIP Advances **7**, 025211 (2017); doi: 10.1063/1.4977559
View online: http://dx.doi.org/10.1063/1.4977559
View Table of Contents: http://aip.scitation.org/toc/adv/7/2
Published by the American Institute of Physics

Acoustic metamaterials with coupled local resonators for broadband vibration suppression

Guobiao Hu,[1] Lihua Tang,[1,a] Raj Das,[1] Shiqiao Gao,[2] and Haipeng Liu[2]
[1]*Department of Mechanical Engineering, University of Auckland, Auckland 1010, New Zealand*
[2]*State Key Laboratory of Explosion Science and Technology, Beijing Institute of Technolog, Beijing 100081, China*

(Received 5 December 2016; accepted 13 February 2017; published online 24 February 2017)

This paper investigates a modified acoustic metamaterial system with local resonators coupled through linear springs. The proposed acoustic metamaterial system can provide three band gaps for broadband vibration suppression. First, the band structure of the modified acoustic metamaterial is calculated by using Bloch's theorem under the assumption of infinite lattice. The existence of three band gaps is confirmed in the band structure. Effects of mass and spring parameters on the band gap behaviour of the modified metamaterial are investigated through a dimensionless parametric study. Based on the parametric study, optimal dimensionless parameters are proposed to achieve maximal total band gap width in the low frequency range. Subsequently, a more realistic finite lattice model is established. The transmittances of the conventional and modified metamaterial systems are compared. The three band gaps predicted from transmittances and broadband vibration suppression behaviour are consistent with the predictions from infinite lattice model using Bloch's theorem. Finally, the time-domain responses are simulated and the superiority of the modified acoustic metamaterial over the conventional one is demonstrated. [http://dx.doi.org/10.1063/1.4977559]

I. INTRODUCTION

Acoustic metamaterial proposed in recent years is a kind of artificial material with exotic properties. The development of acoustic metamaterial was inspired by photonic crystals[1] due to the similarity between acoustic waves and electromagnetic waves.[2] The latter has been widely used in cloaking devices,[3] microwave communications,[4] etc. In analogy to photonic crystal, acoustic metamaterial is often termed as "locally resonant phononic crystal",[2] where "locally resonant" is added in order to distinguish it from the Bragg Scattering phononic crystal[5] that was proposed based on a different mechanism about two decades ago. Some researchers use the term "acoustic metamaterial" specifically referring to "locally resonant phononic crystal", while others extend the scope of acoustic metamaterials and include Bragg Scattering phononic crystal as well. There is no universally accepted definition of acoustic metamaterials to date. In order to avoid misleading the readers, except in the comparative discussions on the locally resonant phononic crystal and the Bragg Scattering phononic crystal in this introduction section, only the term "acoustic metamaterial" or for short "metamaterial" is used in the main content of the paper and it refers to "locally resonant phononic crystals".

Conventional locally resonant phononic crystal has a periodic diatomic microstructure. It is featured by periodically distributed local resonators inside micro-structures. This feature imparts it unique properties that are not easily achieved in natural materials, such as negative effective mass

[a]Author to whom correspondence should be addressed. Electronic mail: l.tang@auckland.ac.nz

density,[6] negative refractive index,[5,7–9] etc. Numerous research interests have been attracted to the band gap phenomenon[10,11] derived from the out-of-phase motion of the introduced local resonators when vibrations occur near resonance. Vibrations of the main structure within the frequency range around the resonant frequency of the local resonator are absorbed and attenuated. The frequency range within which vibrations are attenuated is termed band gap. Many researchers proposed and explored practical applications of acoustic metamaterials by utilizing this feature for vibration suppression,[12,13] sound isolation[14] and wave guiding.[15] Though the aforementioned Bragg Scattering phononic crystal can also generate band gaps when the Bragg Scattering requirement is satisfied, the generation of band gaps strongly depends on the size of the periodic constant.[16] Due to this limitation, with the increase of the wavelength of incident waves, the size of the periodic constant of the desirable Bragg Scattering phononic crystal and thus the overall dimensions of the device has to be increased accordingly. Different from the Bragg Scattering phononic crystal, the locally resonant phononic crystal generates band gaps irrelevant to the periodic constant[10,17] as the mechanism of its band gap generation is similar to that of vibration absorbers. The widely used mass-spring model[10,18] can help understand its operation principle.

Without the size limitation, the locally resonant phononic crystal for vibration suppression has been extensively studied in recent years. Huang *et al.*[19] represented the acoustic metamaterial by using a lattice model consisting of mass-in-mass unit cells. Based on the lattice model, their study showed that the effective frequency-dependent mass density of the acoustic metamaterial could be negative near resonance, which corresponded to the band gap. Yao *et al.*[6] used aluminium blocks and real springs to build a prototype that represented the mass-spring lumped model of acoustic metamaterials. They experimentally confirmed the negative effective mass property and observed the low transmittance of the system in the negative effective mass range. Nouh *et al.*[20] proposed a physical realization of acoustic metamaterials by using beams and plates. A finite element model was developed to predict the properties of the proposed acoustic metamaterial system and experiments were conducted to validate the results from the finite element model. Both simulation and experiment validated the band gap and vibration suppression capacity of the proposed system.

The aforementioned studies mainly focused on the fundamental mechanism of acoustic metamaterials. Other researchers attempted to explore the ways to widen the band gap of acoustic metamaterials or make it tuneable. Huang and Sun[10] proposed the concept of multi-resonator acoustic metamaterials in which each unit cell of the lattice model consists of three masses connected in series by linear springs. It was demonstrated that with the introduced additional inner resonators, more than one band gap appears. Chen *et al.*[21] presented a theoretical study of band gap control of acoustic metamaterials through the use of negative capacitance shunted piezoelectric elements. They connected the inner mass to the outer mass in one unit cell by a piezoelectric element that is shunted to a negative capacitance circuit. In this way, the tunability of the band gap was achieved as the effective stiffness of the piezoelectric element can be changed via the controllable negative capacitance. To the best knowledge of the authors, these are the only two methods reported in the literature to widen the band gaps of acoustic metamaterials. Several other papers presented subsequent works based on the same concepts.[18,22]

In this study, we propose a modified acoustic metamaterial system with local resonators (inner masses) coupled by springs. Such system is proposed for the first time in the field of metamaterial. Without adding extra masses, the proposed acoustic metamaterial system can provide multiple band gaps. Mathematical models are established based on the widely used mass-spring lattice model. First, Bloch's theorem is adopted to derive the solution of an infinite lattice model and the band structure of the modified acoustic metamaterial is compared with that of the conventional one. A parametric study is then conducted to investigate the effects of mass and spring parameters on the band gap behaviour in the presence of coupled inner masses. Subsequently, a more realistic finite lattice model is established and the transmittance is calculated by Laplace transform. The band gaps observed in the transmittance of the system agree well with the prediction of the infinite lattice model using Bloch's theorem. Finally, to validate the superior vibration suppression ability of the proposed metamaterial, numerical simulations are conducted. The time-domain responses of the system under multi-frequency and broadband chirp excitations are investigated. Compared to the performances of a conventional metamaterial system and a simplest mass array system under the same excitations,

the superior vibration suppression ability of the modified acoustic metamaterial is confirmed, which results from the three band gaps by coupling its local resonators.

II. MODIFIED METAMATERIALS WITH INFINITE LATTICE

A. Infinite lattice model of conventional metamaterials

A mass-spring infinite lattice model is often used to represent conventional acoustic metamaterials,[19] which is briefly reviewed in this section.

As shown in FIG. 1, conventional acoustic metamaterials can be represented in the form of an infinite lattice structure consisting of masses and springs. Each unit cell consists of an outer mass m_1 and an inner mass m_2. m_1 and m_2 interact with each other via an inner spring k_2. Two neighbouring unit cells interact with each other via an outer spring k_1. The unit cells are uniformly placed with a periodic distance constant L. Given a harmonic wave propagating in this system, the equations of motion of the i-th unit cell can be derived as

$$\begin{cases} m_1 \frac{d^2 u_1^{(i)}}{dt^2} + k_1 \left(2u_1^{(i)} - u_1^{(i-1)} - u_1^{(i+1)}\right) + k_2 \left(u_1^{(i)} - u_2^{(i)}\right) = 0 \\ m_2 \frac{d^2 u_2^{(i)}}{dt^2} + k_2 \left(u_2^{(i)} - u_1^{(i)}\right) = 0 \end{cases} \tag{1}$$

where u_1 and u_2 represent the displacements of the outer m_1 and inner mass m_2, respectively. Based on Bloch's theorem, the harmonic wave solutions of the i-th and the $(i+n)$-th unit cells are written as

$$\begin{cases} u_\theta^{(i)} = B_\theta e^{j(qx-\omega t)} \\ u_\theta^{(i+n)} = B_\theta e^{j(qx+nqL-\omega t)} \end{cases} \tag{2}$$

where the subscript $\theta = 1, 2$, B_θ is complex wave amplitude, q is the wave number and ω is the angular frequency. Substituting Eq.(2) into Eq.(1) yields

$$\begin{bmatrix} 2k_1 (1 - \cos qL) + k_2 - m_1\omega^2 & -k_2 \\ -k_2 & k_2 - m_2\omega^2 \end{bmatrix} \begin{bmatrix} B_1 \\ B_2 \end{bmatrix} = \begin{bmatrix} 0 \\ 0 \end{bmatrix}. \tag{3}$$

In order to have a non-trivial solution, the determinant of the coefficient matrix of Eq.(3) has to be zero. By expanding the determinant of the coefficient matrix and letting it to be zero, we obtain the dispersion equation as

$$m_1 m_2 \omega^4 - \left[k_2 (m_1 + m_2) + 2k_1 m_2 (1 - \cos qL)\right] \omega^2 + 2k_1 k_2 (1 - \cos qL) = 0. \tag{4}$$

The band structure of conventional metamaterials is obtained by seeking the solution of angular frequency ω with varying qL. Two branches corresponding to two different positive real solutions will appear in the band structure. The gap between these two branches is band gap. It represents a range of frequency within which no positive real solution of ω exists for any qL.

B. Infinite lattice model of modified metamaterials

For conventional metamaterials, there are only 2 positive real solutions (i.e., two branches in the band structure). This is foredoomed by the order of the dispersion equation (Eq.(4)). As a result, only one band gap exists between these two branches.

To have more band gaps, a modified metamaterial system is proposed as shown in FIG. 2. In the proposed system, the inner masses are coupled by linear springs of K. In this way, we allow the interactions between inner masses, which is different from conventional metamaterials. It is worth

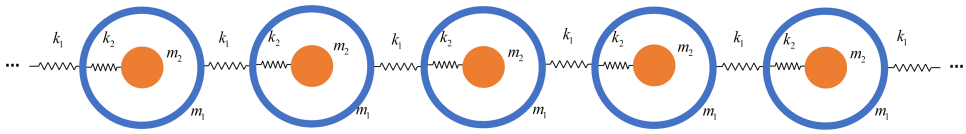

FIG. 1. Infinite lattice model of conventional acoustic metamaterials.

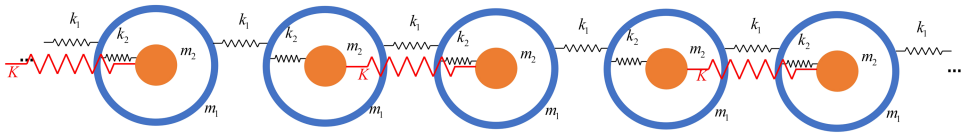

FIG. 2. Infinite lattice model of modified acoustic metamaterials.

noting that instead of connecting all the inner masses one by one, we connect the inner masses alternately. In other words, every two unit cells form a group and the two inner masses in the group are connected. There is no spring K between the groups.

Considering simple harmonic motions of masses in the $(i+1)$-th group, we obtain the equations of motion as

$$\begin{cases} m_1 \frac{d^2 u_1^{(2i+1)}}{dt^2} + k_1\left(2u_1^{(2i+1)} - u_1^{(2i)} - u_1^{(2i+2)}\right) + k_2\left(u_1^{(2i+1)} - u_2^{(2i+1)}\right) = 0 \\ m_2 \frac{d^2 u_2^{(2i+1)}}{dt^2} + k_2\left(u_2^{(2i+1)} - u_1^{(2i+1)}\right) + K\left(u_2^{(2i+1)} - u_2^{(2i+2)}\right) = 0 \\ m_1 \frac{d^2 u_1^{(2i+2)}}{dt^2} + k_1\left(2u_1^{(2i+2)} - u_1^{(2i+1)} - u_1^{(2i+3)}\right) + k_2\left(u_1^{(2i+2)} - u_2^{(2i+2)}\right) = 0 \\ m_2 \frac{d^2 u_2^{(2i+2)}}{dt^2} + k_2\left(u_2^{(2i+2)} - u_1^{(2i+2)}\right) + K\left(u_2^{(2i+2)} - u_2^{(2i+1)}\right) = 0 \end{cases} \tag{5}$$

where $u_1^{(k)}$ and $u_2^{(k)}$ represent the displacements of the outer and inner masses in the k-th unit cell, respectively. The superscript $k = 2i+1, 2i+2$, denotes the two neighbouring unit cells in the $(i+1)$-th group. Based on Bloch's theorem, the wave form of the harmonic displacements of masses in the $(2i+1)$-th and $(2i+2)$-th unit cells are:

$$\begin{cases} u_1^{(2i+1)} = Ae^{j(qx-\omega t)} \\ u_1^{(2i+2)} = Be^{j(qx+qL-\omega t)} \\ u_2^{(2i+1)} = Ce^{j(qx-\omega t)} \\ u_2^{(2i+2)} = De^{j(qx+qL-\omega t)} \end{cases} \tag{6}$$

where A, B, C, D are complex wave amplitudes. Substituting Eq.(6) into Eq.(5) yields

$$\begin{bmatrix} 2k_1 + k_2 - m_1\omega^2 & -2k_1\cos qL & -k_2 & 0 \\ -k_2 & 0 & k_2 + K - m_2\omega^2 & -Ke^{jqL} \\ -2k_1\cos qL & 2k_1 + k_2 - m_1\omega^2 & 0 & -k_2 \\ 0 & -k_2 & -Ke^{-jqL} & k_2 + K - m_2\omega^2 \end{bmatrix} \begin{bmatrix} A \\ B \\ C \\ D \end{bmatrix} = \begin{bmatrix} 0 \\ 0 \\ 0 \\ 0 \end{bmatrix}. \tag{7}$$

The dispersion relation can be derived by setting the determinant of the coefficient matrix of Eq.(7) to be zero, which is the prerequisite for having a nontrivial solution from Eq.(7). This leads to the dispersion equation as

$$\begin{aligned} &-m_1^2 m_2^2 \omega^8 + \left(2Km_1^2 m_2 + 4k_1 m_1 m_2^2 + 2k_2 m_1 m_2^2\right)\omega^6 + \left(4k_1^2 m_2^2 \cos^2(qL) - 8Kk_1 m_1 m_2\right. \\ &\left. -2Kk_2 m_1^2 - 4Kk_2 m_1 m_2 - 4k_1^2 m_2^2 - 8k_1 k_2 m_1 m_2 - 4k_1 k_2 m_2^2 - k_2^2 m_1^2 - 2k_2^2 m_1 m_2 - k_2^2 m_2^2\right)\omega^4 \\ &+\left(-8Kk_1^2 k_2 \cos^2(qL) - 8k_1 k_2 m_2 \cos^2(qL) + 8Kk_1^2 m_2 + 8Kk_1 k_2 m_1 + 8Kk_1 k_2 m_2 + 2Kk_2^2 m_1\right. \\ &\left. + 2Kk_2^2 m_2 + 8k_1^2 k_2 m_2 + 4k_1 k_2^2 m_1 + 4k_1 k_2^2 m_2\right)\omega^2 + 2Kk_1 k_2^2 \cos^2(qL) + 8Kk_1^2 k_2 \cos(qL) \\ &+ 4k_1^2 k_2^2 \cos^2(qL) - 8Kk_1^2 k_2 - 4Kk_1 k_2^2 - 4k_1^2 k_2^2 = 0. \end{aligned} \tag{8}$$

Eq.(8) is an even function of ω of 8-th order. Therefore, for each given wave number q, there should exist at least four non-negative solutions. Note that, for angular frequency ω, only real solutions are sensible. Complex solutions represent evanescent waves whose energy quickly decreases with the wave propagation. Thus, it can be speculated that there exist four branches corresponding to those four positive real solutions in the dispersion curves, which will form three band gaps between the four branches.

C. Band gap behaviour of modified metamaterials

To illustrate the existence of three band gaps of the modified metamaterial, an example with parameters $m_1 = 0.056$ kg, $m_2 = 0.028$ kg, $k_1 = 150$ N/m, $k_2 = 70$ N/m, $K = 105$ N/m are given. FIGS. 3(a) and (b) demonstrate the dimensionless dispersion curves of the conventional and modified metamaterials, respectively. It can be observed that for the modified metamaterial, there appear four branches and three band gaps as expected in the band structure. This indicates that the modified metamaterial could be effective in attenuating vibrations in a broader frequency range than the conventional one. It is worth mentioning that though more than one band gap can be achieved in multi-resonator metamaterial model,[8] additional resonators will increase the weight of the whole system and may impose some requirements and limitations on the lattice size of metamaterials. The benefit of our proposed modified metamaterial is that multiple band gaps can be achieved with no additional mass.

In the following sections, efforts are devoted to investigating the effects of mass and spring parameters on the band gap behaviour of the proposed modified metamaterial. In order to make the subsequent discussions more general, the parametric study are performed using dimensionless parameters defined as $\mu = m_2/m_1$, $\beta = K/k_2$, and $\alpha = \omega_2/\omega_1$, where $\omega_1 = \sqrt{k_1/m_1}$ and $\omega_2 = \sqrt{k_2/m_2}$.

1. Effects of μ and α on band gap behaviour

The characteristic of local resonators, each of which consists of an inner mass and an inner spring, can influence the band gap behaviour of acoustic metamaterials significantly. The effects of the local resonator on the band gap behaviour of the modified metamaterial are thus investigated in terms of the dimensionless parameters: mass ratio μ and natural frequency ratio α. For conventional metamaterials, effects of these two parameters have been discussed in Ref. 18.

Given $\beta = 1$, FIG. 4 depicts the variation of the total band gap width (TBGW) of the proposed modified metamaterial with the change of μ and α, which is expressed in the dimensionless form ω_{TBGW}/ω_2. Here, TBGW is the sum of widths of all the band gaps and will be used hereinafter. It is noted that within the interested ranges of α and μ, for any μ, an optimal α to achieve maximal TBGW can be found.

Given $\alpha = 1.2$ and $\beta = 1$, FIG. 5 further depicts how the band gaps of the modified metamaterial changes with μ. The variation of the three band gaps is presented in FIG. 5(a) and the calculated dimensionless TBGW is shown in FIG. 5(b). It is noted that an optimal μ around 0.6 can be obtained. Correspondingly, in FIG. 5 (a), the optimal μ appears at the place where three band gaps are almost merged, forming an "aggregated band gap". In addition, as compared to the conventional metamaterial, the dimensionless TBGW of the modified metamaterial is much larger as shown in FIG.5(b). This advantage is pronounced when μ reaches the optimum around

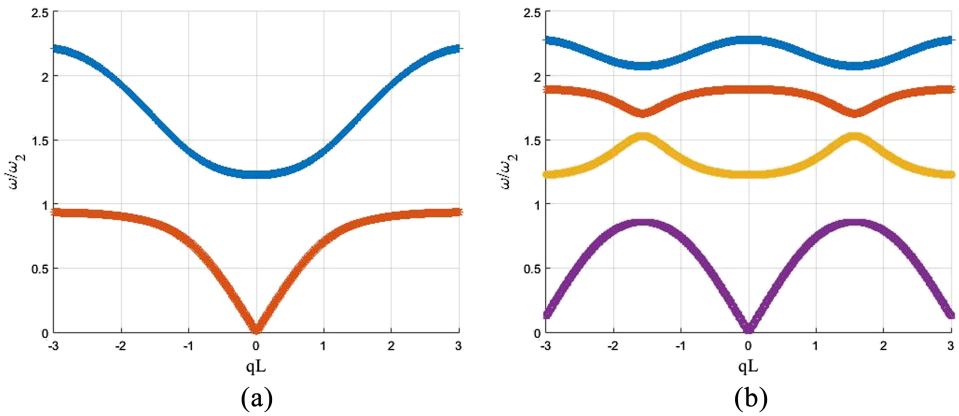

FIG. 3. Band structures of (a) conventional metamateial; (b) modified metamaterial with parameters $m_1 = 0.056$ kg, $m_2 = 0.028$ kg, $k_1 = 150$ N/m, $k_2 = 70$ N/m, $K = 105$ N/m.

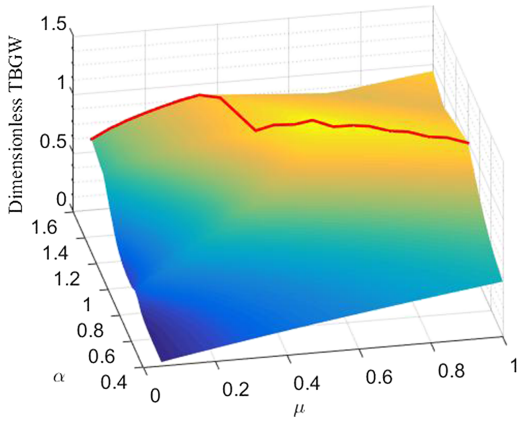

FIG. 4. Dimensionless TBGW versus μ and α ($\beta = 1$).

0.6. Thus the proposed modified metamaterial will provide better broadband vibration suppression performance.

Given $\mu = 0.6$ and $\beta = 1$, FIG. 6 further illustrates how the band gap behaviour changes with α. The variation of the band gap structure and thus the dimensionless TBGW are shown in FIG. 6. From FIG. 6(a), it can be seen that when α is small, the contributions of the second and third band gaps (in pink and light blue) are very minor. Correspondingly, FIG. 6(b) reveals that the dimensionless TBGW of the modified metamaterial is almost the same as that of the conventional one when α is small. The peak of the curve of the modified metamaterial in FIG. 6(b) indicates an optimal α. This optimal α corresponds to the "aggregated band gap" (three band gaps almost merged) shown in FIG. 6(a). It should be noted that the parameters selected to demonstrate the band gap behaviour and the optimal values in FIG. 5 ($\alpha = 1.2$; $\beta = 1$; optimal $\mu \approx 0.6$) and FIG. 6 ($\mu = 0.6$; $\beta = 1$; optimal $\alpha \approx 1.2$) are consistent. In addition, the dimensionless TBGW of the modified metamaterial is always larger than that of the conventional one as shown in FIG. 6(b). By tuning α around optimum, this advantage becomes evident.

2. Effects of β on band gap behaviour

The band gap behaviour of the conventional metamaterial is only dominated by μ and α. While for the modified metamaterial, we have an additional parameter β describing the degree of coupling between inner masses that influences the band gap behaviour.

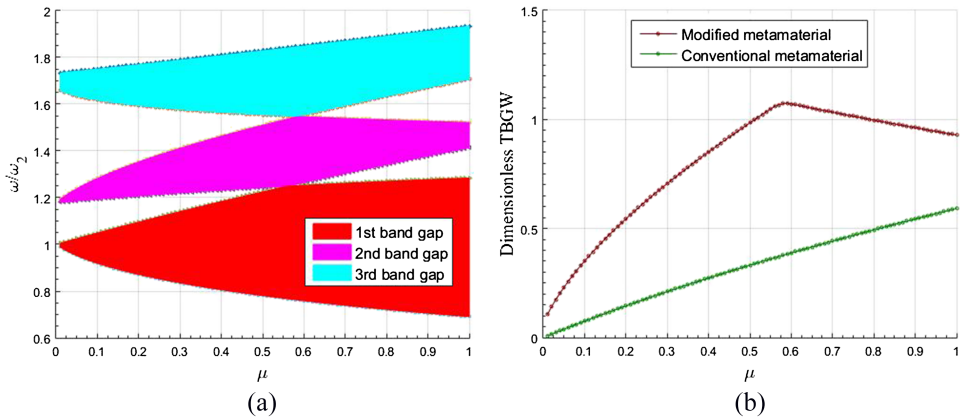

FIG. 5. Band gaps of modified metamaterials versus μ ($\alpha = 1.2$ and $\beta = 1$): (a) distribution of three band gaps; (b) dimensionless TBGW.

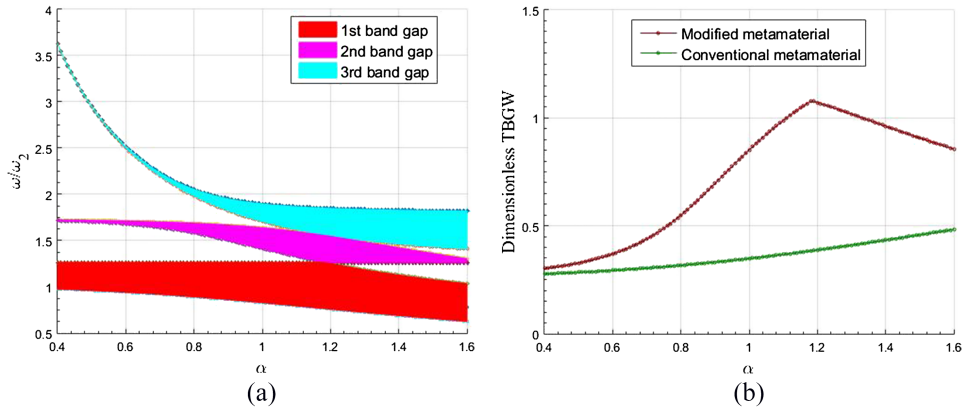

FIG. 6. Band gaps of modified metamaterials versus α (μ = 0.6 and $\beta = 1$): (a) distribution of three band gaps; (b) dimensionless TBGW.

FIG. 7(a) shows the dimensionless TBGW versus μ and β with a fixed $\alpha = 1.2$. It is noted that for any μ (take $\mu = 0.6$ marked by the red line for an example), the TBGW is in general increased with β and there exists a specific β to achieve a local maximal TBGW. Similarly, FIG. 7(b) depicts the dimensionless TBGW versus α and β for a fixed $\mu = 0.6$. For $\alpha > 1$ (take $\alpha = 1.2$ marked by the red line for an example), the TBGW is in general increased with β and there may exist a specific β to achieve a local maximal TBGW.

With $\mu = 0.6$ and $\alpha = 1.2$, FIG. 8 further demonstrate how the band gaps and the dimensionless TBGW change with β. The TBGW of the conventional metamaterial is constant ($\beta = 0$, i.e., no coupling springs K). This is related to the observation that when β is small, the TBGW of the modified metamaterial is close to that of the conventional metamaterial.

We note in FIG. 8(a) that, with the increase of β in the range of $\beta \leq 1.07$, the widths of the first and the third band gaps increase, and the width of the second one initially decreases and then increases. While, when β increases in the range of $\beta > 1.07$, the width of the first band gap does not change and the width of the second one decreases. In this range of $\beta > 1.07$, the increase of the TBGW (as shown in FIG. 8(b)) is mainly from the increase of third band gap. Though it is true that by increasing β in the range of $\beta > 1.07$, the TBGW is increased almost monotonically, the main frequency range of the band gaps (contributed by the 3rd band gap) shifts to the high frequency range. This has no benefit for vibration suppression. The reason is that the wave cannot propagate in the high frequency range anyhow though this is not taken into account in the band gap (for example, ω/ω_2>2.25 in FIG. 3(b)). Additionally, the increase of β when $\beta > 1.07$ even weakens the band gaps

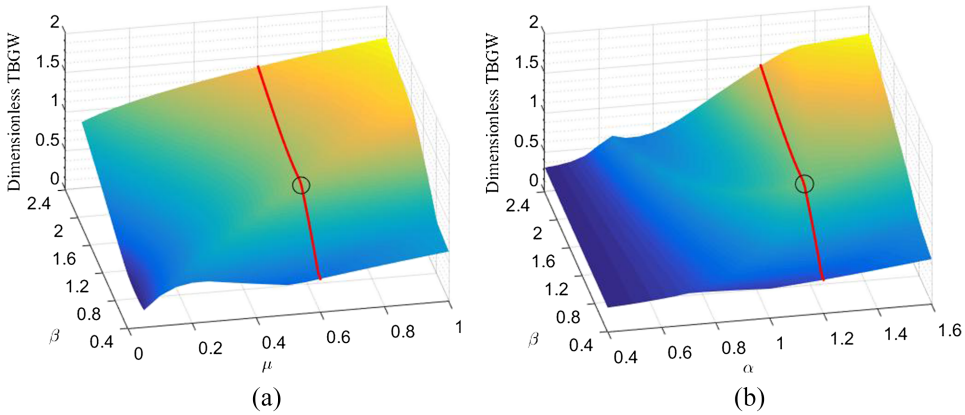

FIG. 7. (a) Dimensionless TBGW versus μ and β ($\alpha = 1.2$); (b) dimensionless TBGW versus α and β ($\mu = 0.6$).

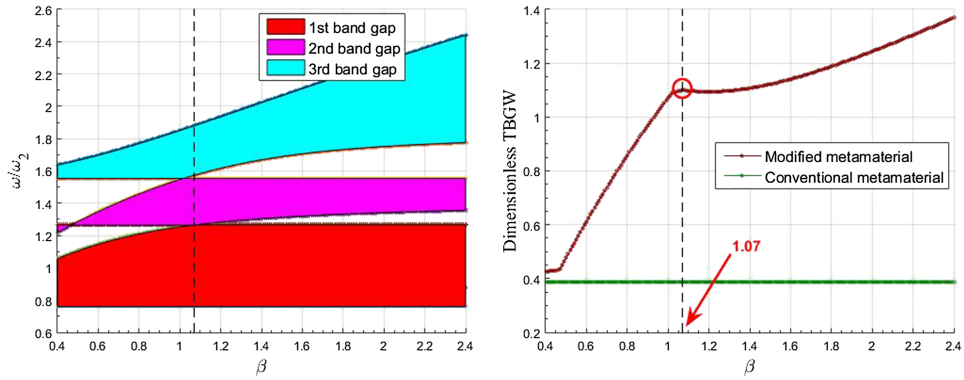

(a) (b)

FIG. 8. Band gaps of modified metamaterials versus β (μ = 0.6 and $\alpha = 1.2$): (a) distribution of three band gaps; (b) dimensionless TBGW.

in the low frequency range, in particular, the second band gap. From this perspective, the attempt to increase the third band gap in the high frequency to increase TBGW with the sacrifice of the band gap width in the low frequency range is not worthwhile. Therefore, $\beta = 1.07$ is regarded as optimal and the three band gaps are nearly merged as an "aggregated band gap".

III. MODIFIED METAMATERIALS WITH FINITE LATTICE

In Section II, the ideal infinite lattice without damping has been adopted, which is the essential assumption of Bloch's theorem. However, the practical systems should be finitely long and with certain energy dissipation mechanism.[23,24] Therefore, it is worth investigating the behaviour of a finite lattice model with damping components as shown in FIG. 9.

The equations of motion of the finite lattice consisting of $2n$ unit cells can be written as

$$\begin{cases} m_1\ddot{u}_1^{(2i+1)} + c_1\left(2\dot{u}_1^{(2i+1)} - \dot{u}_1^{(2i)} - \dot{u}_1^{(2i+2)}\right) + k_1\left(2u_1^{(2i+1)} - u_1^{(2i)} - u_1^{(2i+2)}\right) \\ \qquad + c_2\left(\dot{u}_1^{(2i+1)} - \dot{u}_2^{(2i+1)}\right) + k_2\left(u_1^{(2i+1)} - u_2^{(2i+1)}\right) = 0 \\ m_2\ddot{u}_2^{(2i+1)} + c_2\left(\dot{u}_2^{(2i+1)} - \dot{u}_1^{(2i+1)}\right) + k_2\left(u_2^{(2i+1)} - u_1^{(2i+1)}\right) + K\left(u_2^{(2i+1)} - u_2^{(2i+2)}\right) = 0 \\ m_1\ddot{u}_1^{(2i+2)} + c_1\left(2\dot{u}_1^{(2i+2)} - \dot{u}_1^{(2i+1)} - \dot{u}_1^{(2i+3)}\right) + k_1\left(2u_1^{(2i+2)} - u_1^{(2i+1)} - u_1^{(2i+3)}\right) \\ \qquad + c_2\left(\dot{u}_1^{(2i+2)} - \dot{u}_2^{(2i+2)}\right) + k_2\left(u_1^{(2i+2)} - u_2^{(2i+2)}\right) = 0 \\ m_2\ddot{u}_2^{(2i+2)} + c_2\left(\dot{u}_2^{(2i+2)} - \dot{u}_1^{(2i+2)}\right) + k_2\left(u_2^{(2i+2)} - u_1^{(2i+2)}\right) + K\left(u_2^{(2i+2)} - u_2^{(2i+1)}\right) = 0 \end{cases} \tag{9}$$

where c_1 and c_2 are damping coefficients. The subscripts $2i$+1 and $2i$+2, denotes the two neighbouring unit cells in the (i+1)-th group. Because of the boundary conditions, the governing equations of the first and the last outer masses are given separately as below

$$\begin{cases} m_1\ddot{u}_1^{(1)} + c_1\left(2\dot{u}_1^{(1)} - \dot{u}_0 - \dot{u}_1^{(2)}\right) + k_1\left(2u_1^{(1)} - u_0 - u_1^{(2)}\right) + c_2\left(\dot{u}_1^{(1)} - \dot{u}_2^{(1)}\right) + k_2\left(u_1^{(1)} - u_2^{(1)}\right) = 0 \\ m_1\ddot{u}_1^{(2n)} + c_1\left(\dot{u}_1^{(2n)} - \dot{u}_1^{(2n-1)}\right) + k_1\left(u_1^{(2n)} - u_1^{(2n-1)}\right) + c_2\left(\dot{u}_1^{(2n)} - \dot{u}_2^{(2n)}\right) + k_2\left(u_1^{(2n)} - u_2^{(2n)}\right) = 0 \end{cases} \tag{10}$$

where u_0 is the displacement of the base.

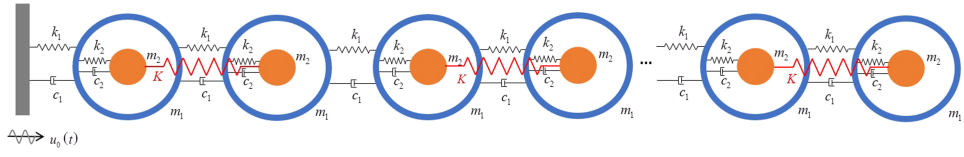

FIG. 9. Finite lattice model of modified acoustic metamaterials.

A. Transmittance of modified metamaterials

Applying the Laplace transform to Eq.(9) and Eq.(10) and setting the Laplace operator $s = j\omega$ (ω is the angular frequency of the excitation), we obtain

$$\begin{cases} -(k_1 + j\omega c_1)U_1^{(2i)} + \left(2k_1 + k_2 - \omega^2 m_1 + 2j\omega c_1 + j\omega c_2\right) U_1^{(2i+1)} \\ \qquad - (k_1 + j\omega c_1)\, U_1^{(2i+2)} - (k_2 + j\omega c_2)\, U_2^{(2i+1)} = 0 \\ -(k_2 + j\omega c_2)\, U_1^{(2i+1)} + \left(k_2 + K - \omega^2 m_2 + j\omega c_2\right) U_2^{(2i+1)} - KU_2^{(2i+2)} = 0 \\ -(k_1 + j\omega c_1)\, U_1^{(2i+1)} + \left(2k_1 + k_2 - \omega^2 m_1 + 2j\omega c_1 + j\omega c_2\right) U_1^{(2i+2)} \\ \qquad -(k_1 + j\omega c_1)\, U_1^{(2i+3)} - (k_2 + j\omega c_2)\, U_2^{(2i+2)} = 0 \\ -(k_2 + j\omega c_2)\, U_1^{(2i+2)} - KU_2^{(2i+1)} + \left(k_2 + K - \omega^2 m_2 + j\omega c_2\right) U_2^{(2i+2)} = 0 \end{cases} \tag{11}$$

$$\begin{cases} \left(2k_1 + k_2 - \omega^2 m_1 + 2j\omega c_1 + j\omega c_2\right) U_1^{(1)} - (k_1 + j\omega c_1)\, U_1^{(2)} - (k_2 + j\omega c_2)\, U_2^{(1)} = (k_1 + j\omega c_1)\, U_0 \\ -(k_1 + j\omega c_1)\, U_1^{(2n-1)} + \left(k_1 + k_2 - \omega^2 m_1 + j\omega c_1 + j\omega c_2\right) U_1^{(2n)} - (k_2 + j\omega c_2)\, U_2^{(2n)} = 0 \end{cases} \tag{12}$$

Defining a set of dimensionless parameters

$$\omega_1 = \sqrt{k_1/m_1};\ \omega_2 = \sqrt{k_2/m_2};\ \zeta_1 = \frac{c_1}{2\sqrt{k_1 m_1}};\ \zeta_2 = \frac{c_2}{2\sqrt{k_2 m_2}};\ \mu = \frac{m_2}{m_1};\ \alpha = \frac{\omega_2}{\omega_1};\ \beta = \frac{K}{k_2};\ \Omega = \frac{\omega}{\omega_2}$$

and substituting them into Eq.(11) and Eq.(12), we obtain their dimensionless forms as

$$\begin{cases} -(1 + 2j\alpha\Omega\zeta_1)\, U_1^{(2i)} + \left(2 + \mu\alpha^2 - \alpha^2\Omega^2 + 4j\alpha\Omega\zeta_1 + 2j\mu\Omega\alpha^2\zeta_2\right) U_1^{(2i+1)} \\ \qquad - (1 + 2j\alpha\Omega\zeta_1)\, U_1^{(2i+2)} - \left(\mu\alpha^2 + 2j\mu\Omega\alpha^2\zeta_2\right) U_1^{(2i+1)} = 0 \\ -\left(\mu\alpha^2 + 2j\mu\Omega\alpha^2\zeta_2\right) U_1^{(2i+1)} + \left(\mu\alpha^2 + \beta\mu\alpha^2 + \beta\mu\alpha^2 - \mu\alpha^2\Omega^2 \right. \\ \qquad \left. + 2j\mu\Omega\alpha^2\zeta_2\right) U_2^{(2i+1)} - \beta\mu\alpha^2 U_2^{(2i+2)} = 0 \\ -(1 + 2j\alpha\Omega\zeta_1)\, U_1^{(2i+1)} + \left(2 + \mu\alpha^2 - \alpha^2\Omega^2 + 4j\alpha\Omega\zeta_1 + 2j\mu\Omega\alpha^2\zeta_2\right) U_1^{(2i+2)} \\ \qquad - (1 + 2j\alpha\Omega\zeta_1)\, U_1^{(2i+3)} - \left(\mu\alpha^2 + 2j\mu\Omega\alpha^2\zeta_2\right) U_1^{(2i+2)} = 0 \\ -\left(\mu\alpha^2 + 2j\mu\Omega\alpha^2\zeta_2\right) U_1^{(2i+2)} - \beta\mu\alpha^2 U_2^{(2i+1)} + \left(\mu\alpha^2 + \beta\mu\alpha^2 + \beta\mu\alpha^2 \right. \\ \qquad \left. - \mu\alpha^2\Omega^2 + 2j\mu\Omega\alpha^2\zeta_2\right) U_2^{(2i+2)} = 0 \end{cases} \tag{13}$$

$$\begin{cases} \left(2 + \mu\alpha^2 - \alpha^2\Omega^2 + 4j\alpha\Omega\zeta_1 + 2j\mu\Omega\alpha^2\zeta_2\right) U_1^{(1)} - (1 + 2j\alpha\Omega\zeta_1)\, U_1^{(2)} \\ \qquad - \left(\mu\alpha^2 + 2j\mu\Omega\alpha^2\zeta_2\right) U_2^{(1)} = (1 + 2j\alpha\Omega\zeta_1)\, U_0 \\ -(1 + 2j\alpha\Omega\zeta_1)\, U_1^{(2n-1)} + \left(1 + \mu\alpha^2 - \alpha^2\Omega^2 + 2j\alpha\Omega\zeta_1 + 2j\mu\Omega\alpha^2\zeta_2\right) U_1^{(2n)} \\ \qquad - \left(\mu\alpha^2 + 2j\mu\Omega\alpha^2\zeta_2\right) U_2^{2n} = 0 \end{cases} \tag{14}$$

where $U_1^{(k)}$ and $U_2^{(k)}$ denote the displacements of the outer and inner masses of the k-th unit cell ($k = 1, 2, \ldots, 2n$), respectively. The transmittance through the system is defined as

$$\tau = 2\log\left|\frac{U_1^{(2n)}}{U_0}\right| \tag{15}$$

which is the ratio of the displacement of the outer mass in the last unit cell to the base displacement.

Given $\mu = 0.6$, $\alpha = 1.2$ and $\zeta_1 = \zeta_2 = 0.008$, the transmittance of a system consisting of 10 unit cells (5 groups of unit cells with coupling springs) is calculated for different β as shown in FIG. 10(a).

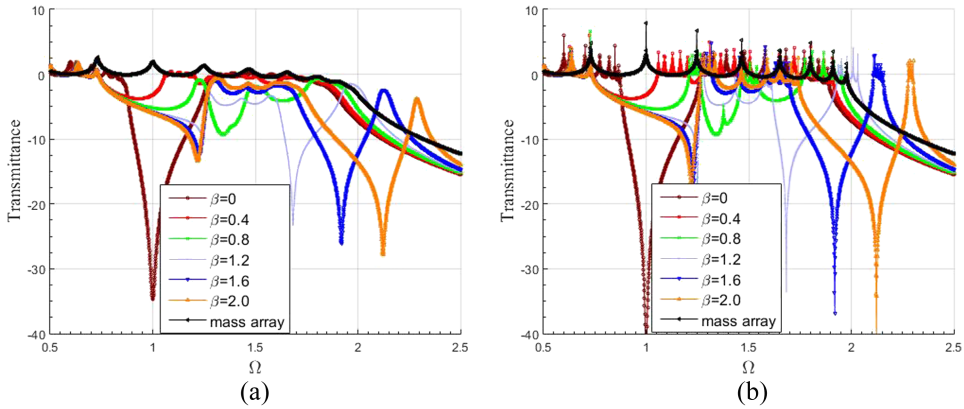

FIG. 10. Transmittance for different β ($\mu = 0.6$ and $\alpha = 1.2$): (a) $\zeta_1 = \zeta_2 = 0.008$; (b) $\zeta_1 = \zeta_2 = 0.000008$.

When $\beta = 0$, there is no coupling springs and the system is exactly the conventional metamaterial. The transmittance of a mass array is also shown in the figure. The mass array is an array of masses (m_1) and springs (k_1) connected in series without any local resonators. It can be seen from FIG. 10(a) that there is no band gap for the mass array system. As expected, there is only one band gap (the sole valley of the brown curve) for conventional metamaterial system ($\beta = 0$). When $\beta \neq 0$, it is noted that multiple band gaps appear for the modified metamaterial system. The transmittance curve is flattened due to the inclusion of damping components.

FIG. 10(b) depicts the transmittance of a system of the same μ and α but with much lighter damping $\zeta_1 = \zeta_2 = 0.000008$. As compared to FIG. 10(a), all the peaks and valleys become much sharper. In addition, for the modified metamaterial system, it is noted in FIG. 10 that with the increase of β, the width of the first band gap initially increases and then keeps constant after β reaches 1.2. The third band gap increases and shifts to the high frequency range. These phenomena have already been predicted in FIG. 8(a) by Bloch's theorem. In the transmittance, though the depth of the first valley of the modified metamaterial system ($\beta \neq 0$) is shallower than that of the conventional one ($\beta = 0$), which indicates that the conventional one would be more effective in attenuating vibrations within the first band gap, the modified metamaterial system has more valleys to suppress vibrations in a much broader frequency range. Besides, the damping effect contradictorily affects vibration suppression inside and outside band gaps (peaks become smaller but the depth of valleys become shallower with a stronger damping).

FIG. 11 further illustrates the correlation between the band structure of the infinite lattice model from Bloch's theorem and the transmittance of the finite lattice model. In this case, the finite lattice model consisting of 100 unit cells ($\mu = 0.6$, $\alpha = 1.2$ and $\zeta_1 = \zeta_2 = 0.000008$). The band structure of the infinite lattice model composed of three band gaps are highlighted in light blue, pink and red, respectively. It can be seen that the range of band gaps can be predicted by either means. With the increase of the number of unit cells in the finite lattice model, the prediction of band gaps from the transmittance is consistent with the band structure predicted from the infinite lattice model by Bloch's theorem.

B. Time-domain responses of modified metamaterials

1. Time-domain response to multi-frequency excitation

In this section, an excitation in the form of $u_0(t) = U_0(\cos(\omega_1 t) + \cos(\omega_2 t))$ is applied to one end of three systems, that is, the mass array system, the conventional metamaterial system and the modified metamaterial system. All of them contain 10 unit cells. At the other end, the vibration displacements of these three systems are compared.

The system parameters used hereinafter for investigation are listed in TABLE I. Note that we intentionally select these system parameters to have $\mu = 0.6$, $\alpha = 1.2$ and $\beta = 1.07$, which are optimal in terms of TBGW according to the discussions in Section II C.

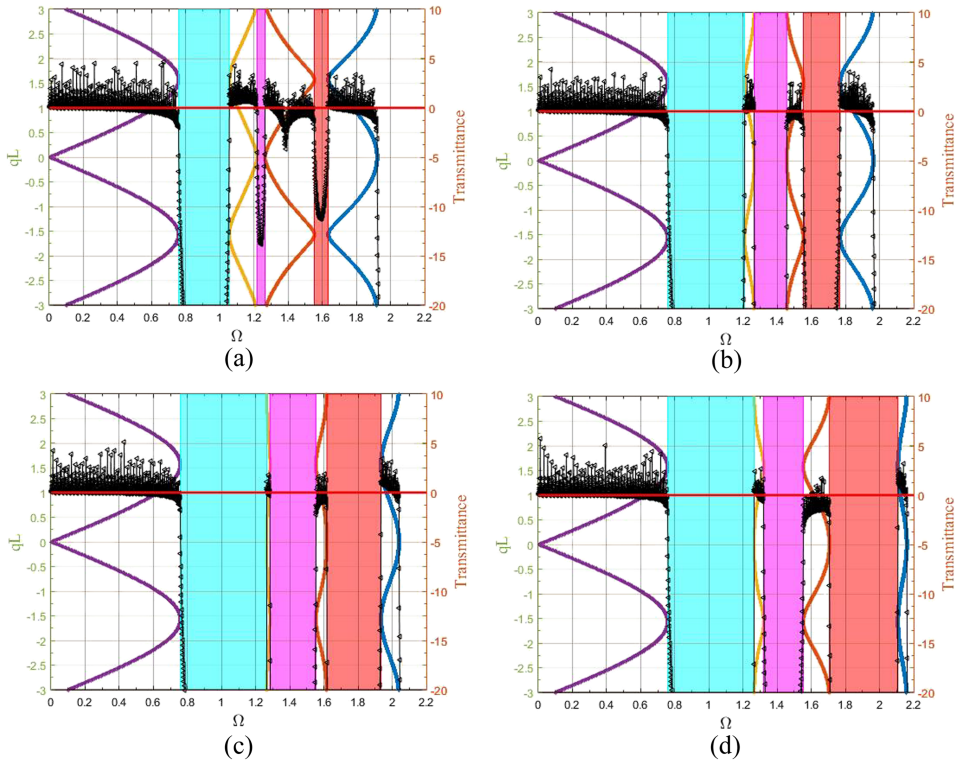

FIG. 11. Band structure of ideal infinite lattice model (left y-axis, band gaps highlighted in light blue, pink and red) and transmittance of finite lattice model with 100 unit cells (right y-axis) (a) $\beta = 0.4$; (b) $\beta = 0.8$; (c) $\beta = 1.2$; (d) $\beta = 1.6$.

The band structures of the conventional and modified metamaterial systems with parameters in TABLE I are shown in FIG. 12. The band gap range of the conventional metamaterial system is [54.46, 78.56] rad/s and the band structure of the modified one contains three gaps: [47.11, 78.54] rad/s, [78.56, 96.48] rad/s and [97.71, 116.68] rad/s.

FIG. 13(a) compares the responses of various systems for the excitation with two frequency components $\omega_1 = 40$ rad/s and $\omega_2 = 80$ rad/s. For the conventional metamaterial system, both ω_1 and ω_2 are out of the band gap range of. For the modified one, ω_1 is out of the band gap range but ω_2 is within the second band gap. Though there is no benefit in terms of vibration amplitude reduction by using either of them, the higher frequency component of ω_2 has been eliminated from the response of the modified metamaterial system.

FIG. 13(b) compares the responses of the three systems for the excitation with two frequency components $\omega_1 = 60$ rad/s and $\omega_2 = 90$ rad/s. For the conventional metamaterial system, ω_1 is within the band gap range while ω_2 is not. For the modified one, ω_1 and ω_2 are within the first and the second band gaps, respectively. In this case, it is noted that the lower frequency component of ω_1 has been

TABLE I. Properties of the systems under investigation.

Parameters	Values	Dimensionless Parameters	Values
m_1	0.056 kg	μ	0.6
m_2	0.0336 kg	α	1.2
k_1	150 N/m	β	1.07
k_2	129.600 N/m	ζ_1	0.008
k	138.672 N/m	ζ_2	0.008
c_1	0.0464 Ns/m		
c_2	0.0334 Ns/m		

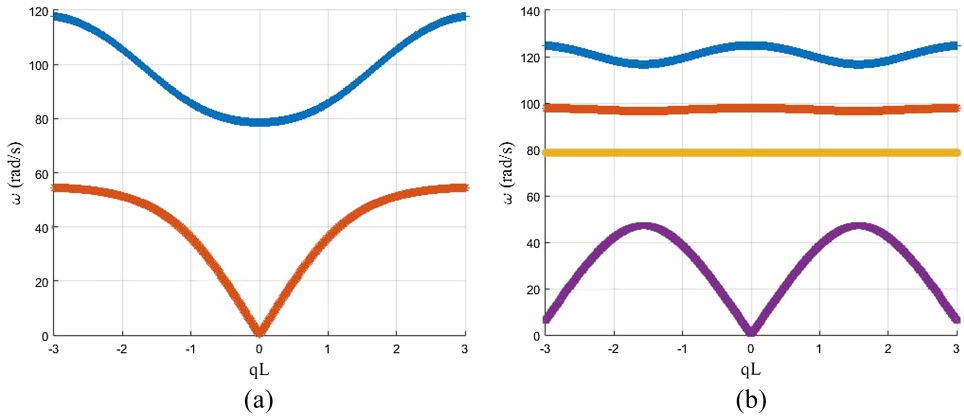

FIG. 12. Band structures of (a) conventional metamaterials; and (b) modified metamaterials.

eliminated from the response of the conventional metamaterial system. The response curve of the modified metamaterial system is almost zero, indicating that both frequency components of ω_1 and ω_2 have been rejected. This demonstrates the superior vibration suppression ability of the modified metamaterial system under multi-frequency excitations, thanks to its multiple band gaps.

2. *Time-domain response to broadband chirp excitation*

For the same systems discussed in the above section, a chirp excitation with frequency from 6 Hz (37.7 rad/s) to 20 Hz (125.7 rad/s) is applied at one end. The magnitude of the acceleration of the chirp is fixed at 2 m/s^2 during the frequency sweep.

The displacement responses of the last outer masses of the conventional and modified metamaterial systems and the last mass of the mass array system are compared in FIG. 14. It is noted that at the beginning, the vibration amplitudes of three systems are high and comparable. Then the vibration amplitudes of both the conventional and the modified metamaterial systems decrease quickly close to zero as the frequency of the chirp enters the band gap of the conventional metamaterial system and the first band gap of the modified metamaterial system. Subsequently, the vibration amplitude of the conventional metamaterial system rebounds significantly since the frequency of the chirp leaves the band gap. The vibration amplitude of the modified metamaterial system stays near zero for a much longer time, benefiting from the existence of its second and third band gaps. Near the end of the sweep duration, the vibration amplitude of

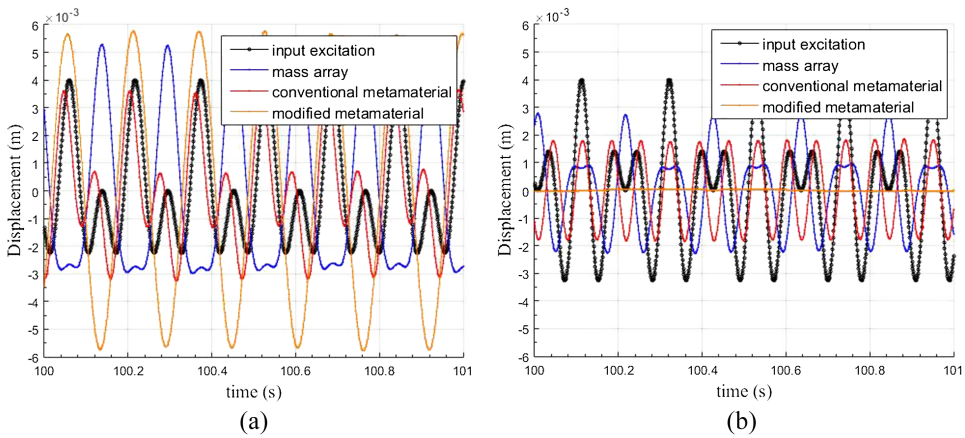

FIG. 13. Displacement responses of various systems due to multi-frequency excitation $u_0(t) = U_0(\cos(\omega_1 t) + \cos(\omega_2 t))$: (a) $\omega_1 = 40$ rad/s and $\omega_2 = 80$ rad/s; (b) $\omega_1 = 60$ rad/s and $\omega_2 = 90$ rad/s.

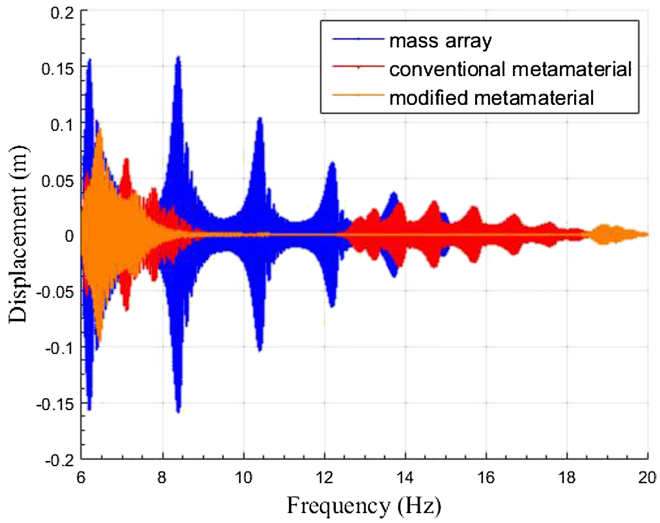

FIG. 14. Displacement responses of various systems due to broadband chirp excitation.

the modified metamaterial system rebounds since the chirp sweeps beyond all the three band gaps.

IV. CONCLUSIONS

This paper has presented a modified acoustic metamaterial system in which the local resonators in the lattice are coupled by springs alternately. It has been demonstrated that the proposed modified metamaterial system can provide three band gaps and attenuate vibrations over a broader frequency range, as compared to conventional metamaterials. Based on the infinite lattice assumption, Bloch's theorem has been used to derive the dispersion relation of the modified metamaterial system. The existence of three band gaps has been observed in the band structure. A dimensionless parametric study has been conducted to investigate the effects of the mass and spring parameters on the band gap behaviour and optimal values of μ, α and β have been proposed.

In addition to the infinite lattice model, the finite lattice model of the modified metamaterial has been established including damping effects. Taking a system consisting of 10 unit cells as an example, the transmittance has been studied. Some phenomena observed in the transmittance are in good agreement with the predictions from the band structure by Bloch's theorem. In the interest of showing the correlation between the infinite and finite lattice models, the transmittance of a lattice consisting of 100 unit cells and the band structure of the infinite lattice model are compared showing the consistency. Apart from the transmittance, the time-domain responses of a mass array, conventional metamaterial and modified metamaterial systems under the same multi-frequency excitation and chirp excitation are compared and the results have verified the superiority of the modified metamaterial system for broadband vibration suppression ability thanks to its multiple band gaps.

ACKNOWLEDGMENTS

This work is financially supported by the Energy Education Trust of New Zealand (no. 3708242) and the PhD scholarship from China Scholarship Council (no. 201608250001).

[1] C. M. Soukoulis, "Photonic band gap materials: the 'semiconductors' of the future?," Physica Scripta **T66**, 146 (1996).
[2] M. H. Lu, L. Feng, and Y. F. Chen, "Phononic crystals and acoustic metamaterials," Materials Today **12**(12), 34–42 (2009).
[3] T. Ergin, N. Stenger, P. Brenner, J. B. Pendry, and M. Wegener, "Three-dimensional invisibility cloak at optical wavelengths," Science **328**(5976), 337–339 (2010).
[4] X. Hu, "Some studies on metamaterial transmission lines and their applications," in *Electrical Engineering* (Royal Institute of Technology, Stockholm, Sweden, 2009).
[5] P. A. Deymier, *Acoustic metamaterials and phononic crystals* (Springer Science & Business Media, 2013), Vol. 173.
[6] S. S. Yao, X. M. Zhou, and G. K. Hu, "Experimental study on negative effective mass in a 1D mass-spring system," New Journal of Physics **10**(4), 043020 (2008).

[7] A. Shelke, S. Banerjee, A. Habib, E. K. Rahani, R. Ahmed, and T. Kundu, "Wave guiding and wave modulation using phononic crystal defects," Journal of Intelligent Material Systems and Structures **25**(13), 1541–1552 (2014).
[8] S. Yang, J. Page, Z. Liu, M. Cowan, C. Chan, and P. Sheng, "Focusing of sound in a 3D phononic crystal," Physical Review Letters **93**(2), 024301 (2004).
[9] J. Xu and J. Tang, "Acoustic prism for continuous beam steering based on piezo-electric metamaterial," in *SPIE Smart Structures and Materials+ Nondestructive Evaluation and Health Monitoring*, 2016, International Society for Optics and Photonics.
[10] G. L. Huang and C. T. Sun, "Band gaps in a multiresonator acoustic metamaterial," Journal of Vibration and Acoustics-Transactions of the Asme **132**(3), 031003 (2010).
[11] S. W. Zhang, J. H. Wu, and Z. P. Hu, "Low-frequency locally resonant band-gaps in phononic crystal plates with periodic spiral resonators," Journal of Applied Physics **113**(16), 163511 (2013).
[12] R. Zhu, X. Liu, G. Hu, C. Sun, and G. Huang, "A chiral elastic metamaterial beam for broadband vibration suppression," Journal of Sound and Vibration **333**(10), 2759–2773 (2014).
[13] J. D. Hobeck and D. J. Inman, "Magnetoelastic metastructures for passive broadband vibration suppression," in *SPIE Smart Structures and Materials+ Nondestructive Evaluation and Health Monitoring*, 2015, International Society for Optics and Photonics.
[14] K. M. Ho, Z. Yang, X. Zhang, and P. Sheng, "Measurements of sound transmission through panels of locally resonant materials between impedance tubes," Applied acoustics **66**(7), 751–765 (2005).
[15] M. Oudich, M. B. Assouar, and Z. L. Hou, "Propagation of acoustic waves and waveguiding in a two-dimensional locally resonant phononic crystal plate," Applied Physics Letters **97**(19), 193503 (2010).
[16] A. Khelif and A. Adibi, *Phononic Crystals: Fundamentals and Applications* (Springer, New York, 2015).
[17] Z. Y. Liu, X. X. Zhang, Y. W. Mao, Y. Y. Zhu, Z. Y. Yang, C. T. Chan, and P. Sheng, "Locally resonant sonic materials," Science **289**(5485), 1734–1736 (2000).
[18] K. T. Tan, H. H. Huang, and C. T. Sun, "Optimizing the band gap of effective mass negativity in acoustic metamaterials," Applied Physics Letters **101**(24), 241902 (2012).
[19] H. H. Huang, C. T. Sun, and G. L. Huang, "On the negative effective mass density in acoustic metamaterials," International Journal of Engineering Science **47**(4), 610–617 (2009).
[20] M. Nouh, O. Aldraihem, and A. Baz, "Wave propagation in metamaterial plates with periodic local resonances," Journal of Sound and Vibration **341**, 53–73 (2015).
[21] Y. Chen, G. Huang, and C. Sun, "Band gap control in an active elastic metamaterial with negative capacitance piezoelectric shunting," Journal of Vibration and Acoustics **136**(6), 061008 (2014).
[22] R. Zhu, Y. Y. Chen, M. V. Barnhart, G. K. Hu, C. T. Sun, and G. L. Huang, "Experimental study of an adaptive elastic metamaterial controlled by electric circuits," Applied Physics Letters **108**(1), 011905 (2016).
[23] J. M. Manimala and C. Sun, "Microstructural design studies for locally dissipative acoustic metamaterials," Journal of Applied Physics **115**(2), 023518 (2014).
[24] M. I. Hussein and M. J. Frazier, "Band structure of phononic crystals with general damping," Journal of Applied Physics **108**(9), 093506 (2010).